Research Inventy: International Journal of Engineering And Science
Vol.15, Issue 5 (May 2025), PP 24-34
Issn (e): 2278-4721, Issn (p):2319-6483, www.researchinventy.com

Design and Implementation of a PSO-Optimized PI Controller in a Quadratic Boost Converter

Muhammad Hisyamudin Ramadhan[1], Iwan Setiawan[2], Susatyo Handoko[3]
[1,2,3] *Department of Electrical Engineering, Faculty of Engineering, Diponegoro University, Jl. Prof. Soedarto, SH, Tembalang, Semarang, Central Java, Indonesia.*
Corresponding Author: hisyamudin.ramadhan99@gmail.com

Abstract: *This study presents the design and implementation of a Particle Swarm Optimization (PSO)-based Proportional-Integral (PI) controller for a Quadratic Boost Converter (QBC) in a closed-loop control system. The PSO algorithm optimize value of the PI controller parameteres (Kp and Ki) using the Integral Time Absolute Error (ITAE) as the objective function to get the most optimize value. In this study, the PSO-based PI controller performance is tested under varying operating conditions such as different voltage reference setpoints which are 240V, 220V, and 180V with a fixed input voltage of 18V. Secondly, different load resistance value (50 Ω, 100 Ω, 200 Ω) also used to verify the controller performance. From the simulation results, shows that the proposed PSO-based PI controller successfully regulates the output voltage to match the reference values accross all the test scenarios. Performance metrics such as settling time, overshoot, and steady-state error are analyzed to validate the designed controller's robustness and dynamic response. According to the results, the PSO-optimized PI controller is a effective option in the case of high-gain DC-DC converter applications since it guarantees precise and steady voltage regulation. The proposed system is simulated in MATLAB/Simulink software to analyse the performance of the system.*

Keywords: *Quadratic Boost Converter, PSO-based PI controller, ITAE objective function, Closed-Loop Control.*

Date of Submission: 01-05-2025 Date of Acceptance: 09-05-2025

I. INTRODUCTION

In the modern era, energy has become a critical factor which leading to a significant increase in the demand for the energy sources. This growing demand, driven by rapid technological advancements and demographic changes, makes it increasingly difficult to meet the energy needs with existing supply sources.

From the case (Essaaidi & El Hani, 2015; Guangul & Chala, 2019; Lofthouse, 2015; Niknam et al., 2011) explain various challenges such as rising electricity demand, fossil fuel depletion, environmental concerns, and the search for alternative energy, have prompted the development of renewable energy power generation. Renewable energy derived from natural resources like solar, wind, water, and geothermal heat, are naturally replenished and can be converted into electricity using different energy conversion methods (2016 IEEE International Conference on Renewable Energy Research and Applications (ICRERA), 2016; Kirubakaran et al., 2009; Trujillo et al., 2016).

Photovoltaic (PV), one of the renewable energy sources are mostly used to generate a clean power, however it has disadvantage such as the powers are intermittent in nature. The electricity produced by photovoltaic (PV) relies heavily on varying solar energy, irradiance, and temperature that affect to the output voltage of the PV panel. Therefore, to ensure a steady power output, a solution such as effective energy storage like supercapacitors, batteries, and fuel cells (FCs) are used. Fuel cells (FCs) are ideal for reliable, continuous power generation but struggle with rapid load changes due to slow electrochemical responses. Their performance depens on power electronic converters, as a single fuel cell produces insufficient voltage for grid integration. While stacking multiple cells in series/parallel increases voltage, but it also reduces efficiency and increase costs.

Power electronic converter such as DC-DC converter is implemented as an interface to step-up the voltage obtained from these systems. The voltage step-up capability of conventional boost converters relies on the duty cycle, while achieving high step-up ratios requires a high duty cycle. To overcome this limitation, various topologies have been explored to achieve higher voltage conversion (Hsieh et al., 2012, 2014; Hu & Gong, 2014; López-Santos et al., 2013; Nouri et al., 2013; Qian et al., 2012).

Among them, the Quadratic Boost Converter (QBC) structurally similar to two cascaded boost converters offering a high voltage conversion ratio and requires only one active switch, useful for improving efficiency (López-Santos et al., 2013). Quadratic Boost Converter is commonly used in high voltage applications like distributed generation system.

Proportional-Integral (PI) control systems are applied in order to improve the QBC performance. The PI controller is widely used in these systems due to its simplicity and effectiveness in maintaining steady-state error within acceptable limits compared to PID (Das et al., 2018). Conventional tuning methods for PI controllers such as Ziegler-Nichols (ZN) often fail to provide the necessary dynamic response and robustness under such varying conditions. The ZN method could be effective for linear and time-invariant systems, but in can lead to aggresive tuning resulting in overshoot, instability, and poor performance in systems with nonlinearities and time-varying dynamics such as those encountered in PV applications.

Therefore, optimization techniques like Particle Swarm Optimization (PSO) have been increasingly used for tuning control systems. PSO is a widely-used optimization algorithm that identifies optimal parameters by allowing a population of particles to self-adapt iteratively improving candidate. PSO has been applied in several studies to optimize PI and PID controllers for various applications, including renewable energy systems(Abdolrasol et al., 2022; Barrios Aguilar et al., 2020; Borin et al., 2019; Liaquat et al., 2019; Malarvili et al., 2021; *Optimization of Electrical and Electronic Equipment (OPTIM), 2014 International Conference On*, 2014; Sahin et al., 2014).

This paper aims to solve the challenge of PSO-based PI controller tuning method in Quadratic Boost Converter to get the optimize *Kp* and *Ki* for the PI controller robustness so that the stable output voltage can meet the set-point. The proposed system is simulated using MATLAB/Simulink software.

II. SYSTEM DESCRIPTION

2.1 Modelling of the Quadratic Boost Converter.

The Quadratic Boost Converter (QBC) is a non-isolated DC-DC converter that offers a higher voltage conversion ratio compared to a conventional boost converter. This is accomplished through the use of two inductors and two capacitors in a coupled configuration, enabling a two-stage voltage boosting mechanism (López-Santos et al., 2013). The enhanced voltage gain provided by the QBC makes it particularly suitable for applications such as photovoltaic (PV) systems, where the input voltage from the PV array must be significantly increased to meet the load and battery requirements. Additionally, the QBC improves efficiency and reduces component stress by distributing the voltage conversion process across two stages. The Quadratic Boost Converter (QBC) shown in Figure 1 utilizes a single active switch, and its operational analysis is conducted based on the state of this switch.

Figure1. Basic Diagram of Quadratic Boost Converter

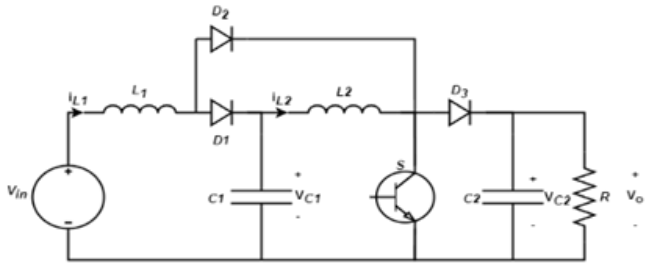

2.1.1 Continuous Conduction Mode (CCM) Switch ON

When the switch "S" is activated the time interval becomes [t_o,t_{on}]. Figure 2 shows the structure of a quadratic boost converter when the switch is in active mode.

Figure*2*. Basic Diagram of Quadratic Boost Converter in Activated Mode

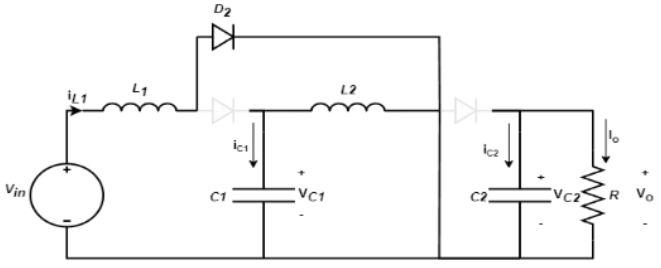

The current flowing through L_1 forces the conduction of diode D_2 while diodes D_1 and D_3 are blocked. In this mode, the two inductors L_1 and L_2 are charged by the input voltage V_{in} and V_{c1} respectively while I_{L1} and I_{L2} increase from I_{min} to I_{max}. The charging current i_o is supplied by capacitor C_2.

The differential equations for the state variables are as follows when the switch is closed.

$$\Delta iL_1 = \frac{V_i}{L_1} \quad (1)$$

$$\Delta iL_2 = \frac{V_{C1}}{L_2} \quad (2)$$

$$\Delta VC_1 = -\frac{i_{L2}}{C_1} \quad (3)$$

$$\Delta VC_2 = -\frac{V_{out}}{RC_2} \quad (4)$$

ΔiL_1 and ΔiL_2 are the current variations respectively at inductors L_1 and L_2 and ΔVC_1 and ΔVC_2 those of the voltages across C_1 and C_2.

2.1.2 Continuous Conduction Mode (CCM) Switch OFF

In this mode, the switch "S" is off and the Diode D_2 is now non-transient while dioded D_1 and D_3 are transient, allowing current to flow through the inductors to charge capacitors C_1 and C_2.

Figure3. Basic Diagram of Quadratic Boost Converter in Deactivated Mode

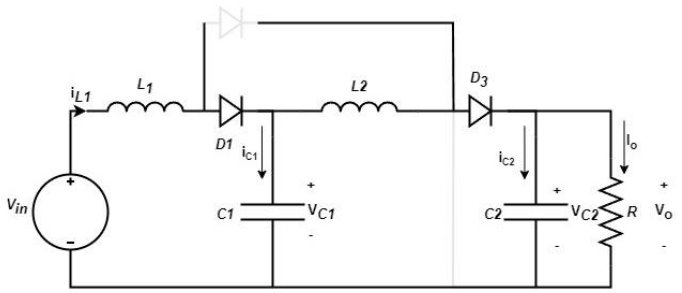

The differential equations relating the state variables when switch S is off are shown below:

$$\Delta iL_1 = \frac{V_i}{L_1} - \frac{V_{C1}}{L_1} \quad (5)$$

$$\Delta iL_2 = \frac{V_{C1}}{L_2} - \frac{V_{out}}{L_2} \quad (6)$$

$$\Delta VC_1 = \frac{i_{L1}}{C_1} - \frac{i_{L2}}{C_1} \quad (7)$$

$$V_{out} = \frac{i_{L2}}{C_2} - \frac{V_{out}}{RC_2} \quad (8)$$

For switching converters, average values are used. The equations are shown below:

$$\Delta iL_1 = \frac{V_i}{L_1} - \frac{V_{C1}}{L_1}(1-D) \quad (9)$$

$$\Delta iL_2 = \frac{V_{C1}}{L_2} - \frac{V_{out}}{L_2}(1-D) \quad (10)$$

$$\Delta VC_1 = \frac{i_{L1}}{C_1}(1-D) - \frac{i_{L2}}{C_1} \quad (11)$$

$$\Delta V_{out} = \frac{i_{L2}}{C_2} - \frac{V_{out}}{RC_2} \quad (12)$$

In the steady state condition, the sum of the voltage for a switching operation should be equal to zero. Therefore, the equations are shown as follows:

1. Inductance L_1

$$\Delta iL_{1(ON)} + \Delta iL_{1(OFF)} = 0 \quad (13)$$

$$VC_1 = \frac{V_i}{1-D} \quad (14)$$

2. Inductance L_2

$$\Delta iL_{2(ON)} + \Delta iL_{2(OFF)} = 0 \quad (15)$$

$$V_{out} = \frac{V_i}{1-D^2} \quad (16)$$

3. Current relations

$$i_{C(ON)} + i_{C(OFF)} = 0 \quad (17)$$

$$iL_2 = \frac{i_o}{1-D} \text{ and } iL_1 = \frac{i_o}{1-D^2} \quad (18)$$

The electrical components for the design of quadratic boost converter can be determined from the following relationships:

$$L_1 = \frac{V_{out}(1-D)^2 D}{\Delta iL_1 f} \text{ and } L_2 = \frac{V_{out}(1-D)D}{\Delta iL_2 f} \quad (19)$$

$$C_1 = \frac{i_o D}{(1-D)\Delta V C_1 f} \text{ and } C_2 = \frac{i_o D}{\Delta V C_2 f} \quad (20)$$

In this study, the input voltage V_{in} value is constantly 18 V while the output voltage V_{out} is set to 180 V, 220V, and 240 V respectively following the voltage reference in closed-loop control system. The load of the resistance is set to 50 Ω, 100 Ω, and 200 Ω. The switching frequency is set at 10kHz.

The values of the components are given in Table 1.

Table1.Values of the components used for Quadratic Boost Converter

Parameters	Value
Input voltage (V)	18V
Output voltage (V)	180-240V
R(Ω)	50-200
Duty Cycle	70%
Switching Frequency (Hz)	10kHz
Inductor L_1	1.77µH
Inductor L_2	1.96µH
Capacitor C_1	65.3mF
Capacitor C_2	16.3mF

2.2 Controller Design: PI Controller

The controller serves as the most critical component in any system which is configured to improve the output waveform by adjusting the modulation index control signal. In this study, a feedback control scheme is used to control the output voltage of the Quadratic Boost Converter to a desired value. The PI controller scheme also work to reduces the Steady State Error (E_{ss}) and control the desired voltage output base on the reference voltage (V_{ref}) as a set point.

Figure*4*. Block Diagram of PI Controller

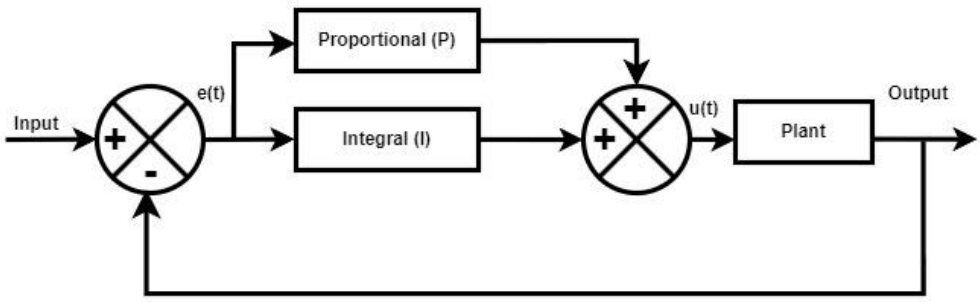

The PI controller aims to achieve a fast response to changes in the setpoint while also ensuring that the process variable eventually settles at the desired setpoint with zero steady-state error. The output of a continuous-time PI controller, denoted as *u*(t) is given by the following equation:

$$u(t) = K_p e(t) + K_i \int_0^t e(\tau)d\tau + u(0) \quad (21)$$

Where:

- *u(t)* is the control signal at time *t*
- *e(t)* is the error signal at time *t*, which defined as the difference between the setpoint *r*(t) and the measured process variable *y(t)*

$$e(t) = r(t)-y(t)$$

- K_p is the proportional gain
- K_i is the integral gain

2.3 PSO Algorithm for PI Controller Optimization

Particle Swarm Optimization (PSO) is a population-based optimization method first developed by Kennedy and Eberhart inspired by the collective behaviour of birds foraging for food. In this algorithm, particles explore a multi-dimensional problem space to find optimal solutions.

PSO algorithm is one of the optimization methods that widely used since it has advantages over the other optimization methods. It has easy implementation, robustness, and globe convergence capability (Abdolrasol et al., 2022). According to these reasons, the PSO algorithm is selected in this study for tuning the K_p and K_i parameters by searching the best values to make the error as small as possible or zero. By using that technique, the optimal value of the objective function can be determined and the algorithm convergence condition may be managed.

PSO algorithm principles are basically depending on two factors which are velocity and position. Velocity is the term used in PSO to describe the rate of positional change with respect to time. Velocity in PSO, then, is the rate at which position is adjusted around the iterations. When the iterations increase by one, the velocity (v) and position (x) dimensions lined up. In order to find novel answers, the system repeatedly explores the d-dimensional issue space (Sinha et al., 2025). The relationship of these factors is represented by using the following equations:

$$V_i^d(t+1) = \omega V_i^d(t) + c_1 r_1 \left(P_i^d(t) - X_i^d(t)\right) + c_2 r_2 \left(P_i^d(t) - X_i^d(t)\right) \quad (22)$$

$$X_i^d(t+1) = X_i^d(t) + V_i^d(t+1) \quad (23)$$

Where, c_1 is a social rate and c_2 is cognitive rate while r_1 and r_2 are the random interval (0,1). V is the velocity, w is the inertia factor, and X is the position factor.

The algorithm is searching for the optimal values for K_p and K_i to improve the PI controller performance. The process will end when the stopping criteria is met. In this study, Integral of Time-weighted Absolute Error (ITAE) criterion, one of commonly used performance index is used as a fitness function or objective function. The selected fitness function mentioned above has been applied to evaluate the performance of the proposed control system to tune controller parameters to minimize the accumulation of errors over time.

In this case, the aim of the PSO algorithm is to find the controller parameters that minimizes the ITAE criteria as an objective function. The ITAE value is computed by integrating the absolute error multiplied by time as shown in the equation below:

$$ITAE = \int_0^{T_{end}} t|\boldsymbol{e(t)}|dt \quad (24)$$

Figure5. Flow Chart of PSO Optimization for Optimal PI Controller Parameter

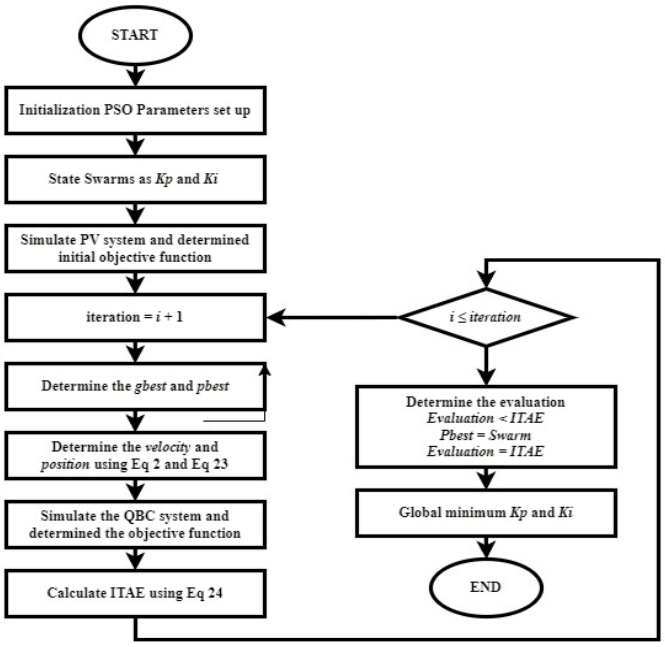

Where the error at time t is represented by $e(t)$, and T_{end} is the simulation end time. A time weighting element prior to integration is incorporated into ITAE, a modified form of IAE (Ahmed et al., 2024a). By prioritizing errors that occur earlier in the time period, it focuses on minimizing the accumulation of absolute errors over time (Ahmed et al., 2024b). The flow chart of proposed PSO optimization algorithm for optimal PI controller parameter is shown in Figure 5. While the iterations result against the ITAE is shown in Figure 6 and the parameters used in the PSO algorithm are given in the Table 2.

Figure*6*. Iterations result againts the ITAE

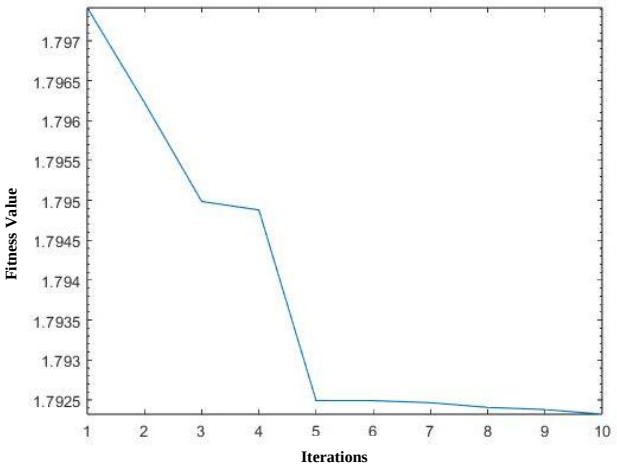

Table*2*.Components of PSO

Parameters	Value
Number of Variables	2
Maximum Iteration	10
Upper Bound (*Kp* & *Ki*)	200, 200
Lower Bound (*Kp* & *Ki*)	0, 0
Number of Particles	10
W Max	0.9
W Min	0.2
C_1	2
C_2	2

III. SIMULATION RESULTS

In this study, the PSO-optimized PI controller for a Quadratic Boost Converter is proposed and simulated in MATLAB/Simulink program. The proposed system as shown in Figure 7, consists of the Quadratic Boost Converter and the PSO-optimized PI controller using ITAE as an objective function which present a robust-optimal control approach for Quadratic Boost Converter that improves it control capability and output voltage error tracking. The proposed control strategy employs an PSO-optimized PI controller using ITAE as an objective function, which used to eliminate oscillations, overshoots, undershoots, and steady-state fluctuations. The QBC and the PSO parameters value are shown in the Table 1 and Table 2 respectively.

This effective control strategy is applied to a Quadratic Boost Converter with a fixed input voltage value, but varying several reference voltage values as set points and also varying the resistance load value to test the performance of the QBC and control system. Hence, to maintain the required output voltage, the system utilizes a PI controller using a closed-loop method. PSO is used to tune the PI controller's gains, making the controller more robust and efficient for smooth operation towards the desired outputs.

To determine the controller's robustness, the performance of the converter is tested under various operating conditions as previously explained. The desired output voltage is set at 180V, 220V, and 240V following the reference voltage as a set point. The resistance load value is set to 50Ω, 100Ω, and 200Ω. The PSO algorithm is running with number of variables set as 2 which are represent K_p and K_i parameter, maximum iterations set as 10, while the number of particles set as 10. The upper and lower bound used as K_p and K_i parameter values are set as 200 and 0 respectively. The inertia constant *w* consists of *w max* and *w min* are given a damping of 0.9 and 0.2 respectively. The acceleration coefficients c_1 and c_2 are both set as 2. Optimiziation is carried out with ITAE and objective function and optimal PI parameters are obtained. It is presumed that the switching loss and other voltage drops across the passive components are minimal. The whole system proposed is shown in Figure 7.

Figure*7*. Simulink Representation of the Whole System

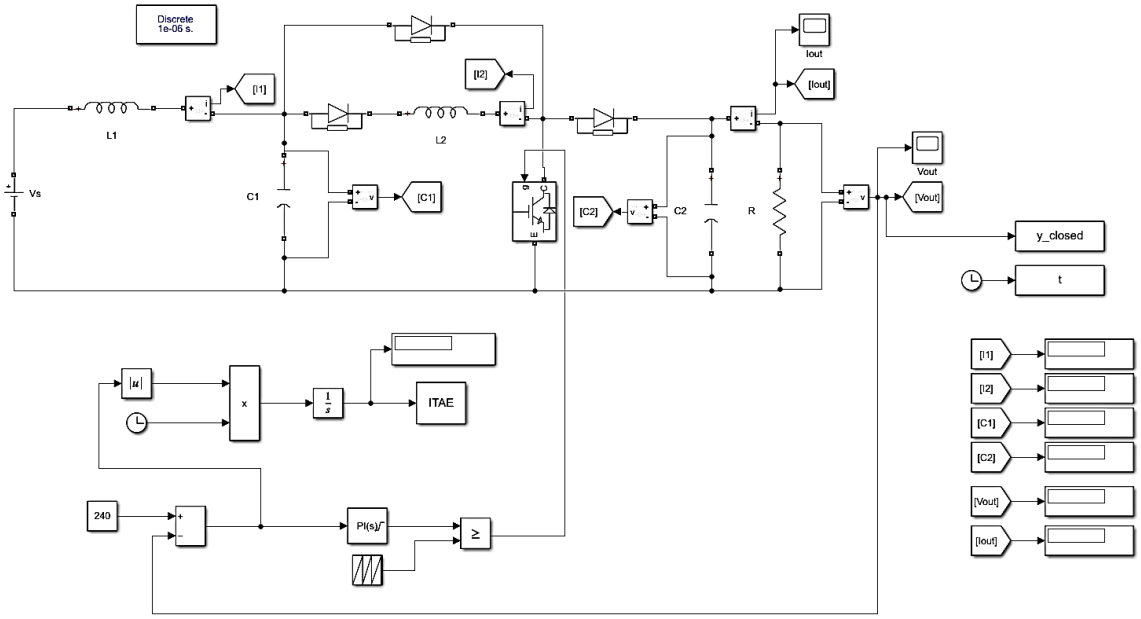

The system is running in MATLAB/Simulink R2021a using discrete simulation type and sample time 1µs. The solver selection is using variable-step and ode23s (stiff/Mod. Rosenbrock) as a solver. The simulation stop is set as 0.8 seconds.

There are three cases carried out in simulation to test the performance quality of the proposed system:

i. The input voltage remains constant at 18V, reference voltage is set as 180V, and the resistance load set as 50Ω, 100Ω, and 200Ω.
ii. The input voltage remains constant at 18V, reference voltage is set as 220V, and the resistance load set as 50Ω, 100Ω, and 200Ω.
iii. The input voltage remains constant at 18V, reference voltage is set as 240V, and the resistance load set as 50Ω, 100Ω, and 200Ω.

By default, the initial value of the resistance value is 100Ω as the settings will be used for the PSO to looking for optimized K_p and K_i parameter. Then, the obtained K_p and K_i value from 100Ω will remain use for 50Ω and 200Ω. The system performance is evaluated based on overshoot, settling time, steady state error and rise time.

3.1. Case 1: Reference Voltage 180V

The first case the reference voltage is set as 180V and default resistance load as 100Ω. From the simulation, PSO algorithm based ITAE objective function obtained fitness value after ten iterations as 0.20183 while the optimized K_p and K_i values are 0.6372 and 120.8912 respectively. The iteration result is shown in Figure 8.

Figure*8*. Iterations result of Case 1

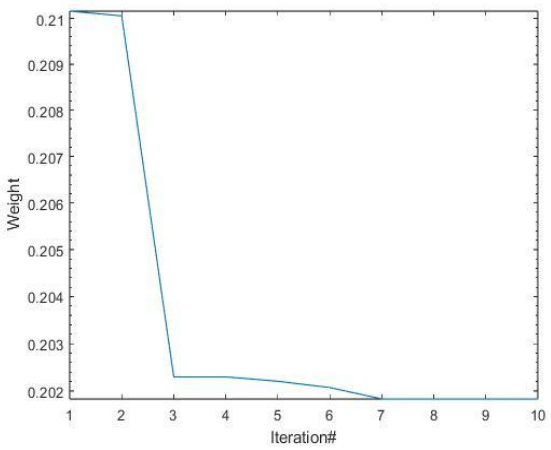

The output voltage results are obtained from each resistance load variations. From the Figure 9 it shows that the output voltage is successfully match the set point 180V. The overshoot, settling time, steady state error and rise time also obtained as shown at Table 3.

Figure9. Output Voltage from 50Ω, 100Ω, and 200Ω Resistance Load Variations

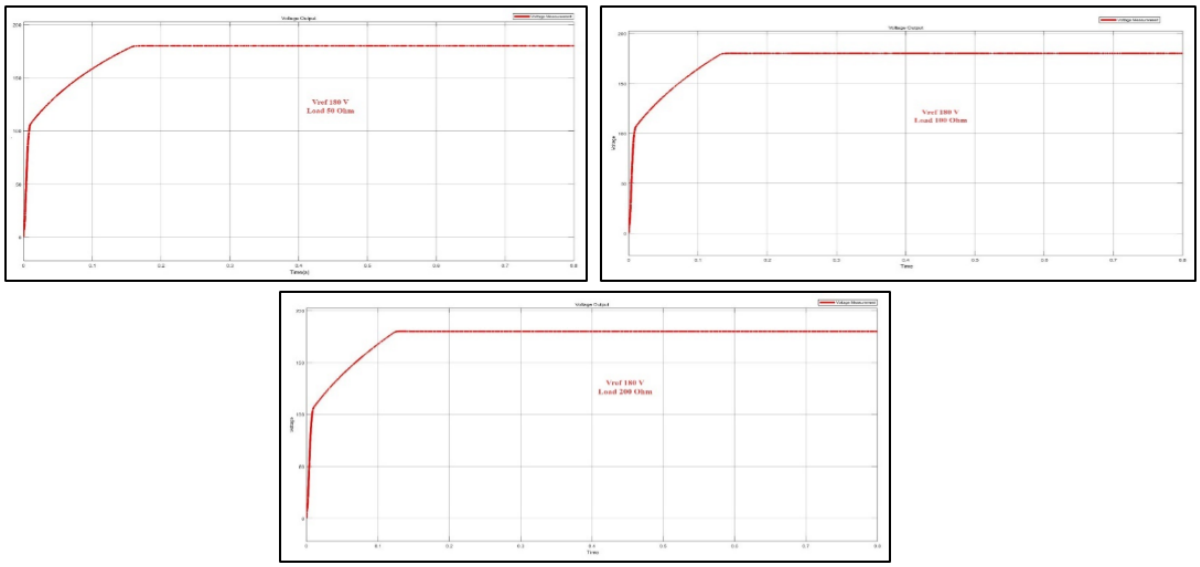

Table3.System Response with Optimized Parameter

Parameters	Voltage Output(V)	Current Output (A)	M_{pp} (%)	E_{ss}(V)	T_{ss}(ms)	T_r(ms)
Vref 180V, Load 50 Ω	180.012	3.6	0.006	0	151.87	105.99
Vref 180V, Load 100 Ω	180.029	1.8	0.161	0	128.62	92.39
Vref 180V, Load 200 Ω	180.065	0.9	0.036	0	119.84	86.99

3.2. Case 2: Reference Voltage 220V

The second case the reference voltage is set as 220V and default resistance load as 100Ω. From the simulation, PSO algorithm based ITAE objective function obtained fitness value after ten iterations as 0.94339 while the optimized Kp and Ki values are 1.5263 and 118.2285 respectively. The iteration result is shown in Figure 10.

Figure10. Iterations result of Case 2

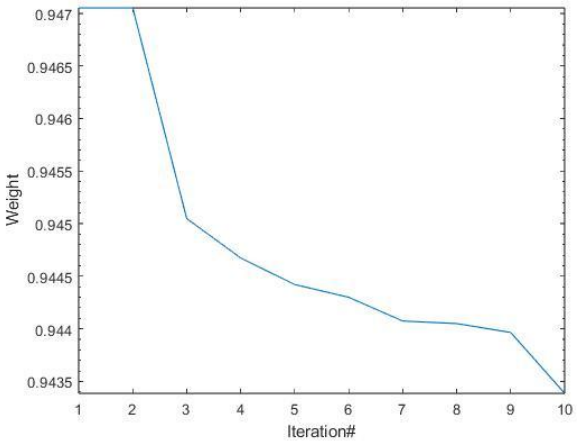

The output voltage results are obtained from each resistance load variations. From the Figure 11 it shows that the output voltage is successfully match the set point 220V. The overshoot, settling time, steady state error and rise time also obtained as shown at Table 4.

Figure*11*. Output Voltage from 50Ω, 100Ω, and 200Ω Resistance Load Variations

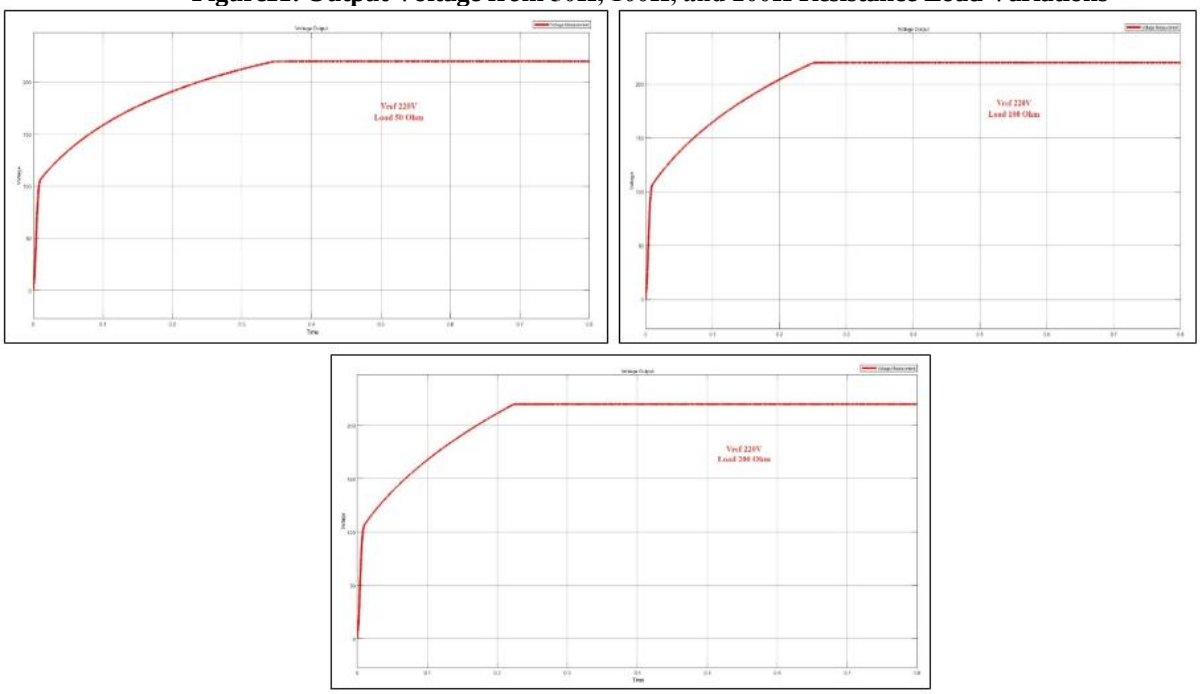

Table*4*. System Response with Optimized Parameter

Parameters	Voltage Output(V)	Current Output (A)	M_{pp} (%)	E_{ss}(V)	T_{ss}(ms)	T_r(ms)
Vref 220V, Load 50 Ω	220.004	3.6	0.001	0	325.78	231.13
Vref 220V, Load 100 Ω	220.007	2.2	0.003	0	241.33	183.39
Vref 220V, Load 200 Ω	220.014	0.9	0.006	0	215.93	167.28

3.3. Case 3: Reference Voltage 240V

The second case the reference voltage is set as 240V and default resistance load as 100Ω. From the simulation, PSO algorithm based ITAE objective function obtained fitness value after ten iterations as 1.7923 while the optimized Kp and Ki values are 133.6885 and 79.1542 respectively. The iteration result is shown in Figure 12.

Figure12. Iterations result of Case 3

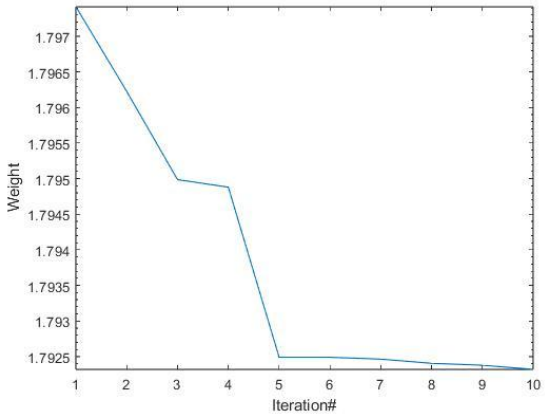

The output voltage results are obtained from each resistance load variations. From the Figure 12 it shows that the output voltage is successfully match the set point 240V. The overshoot, settling time, steady state error and rise time also obtained as shown at Table 5.

Figure*13*. Output Voltage from 50Ω, 100Ω, and 200Ω Resistance Load Variations

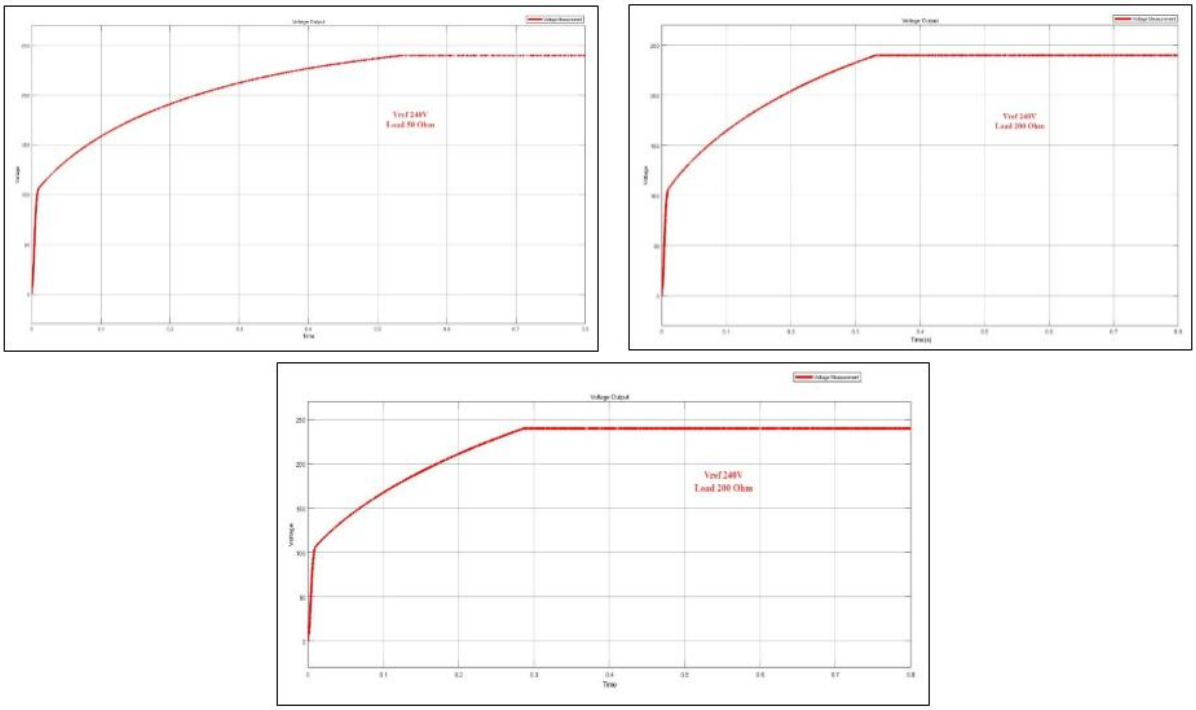

Table*5*. System Response with Optimized Parameter

Parameters	Voltage Output(V)	Current Output (A)	M_{pp} (%)	E_{ss}(V)	T_{ss}(ms)	T_r(ms)
Vref 240V, Load 50 Ω	240.045	4.8	0.019	0	488.06	325.37
Vref 240V, Load 100 Ω	240.139	2.4	0.058	0	317.01	240.10
Vref 240V, Load 200 Ω	240.152	1.2	0.063	0	276.11	214.81

IV. CONCLUSION

This study successfully designed and implemented a PSO-optimized PI controller for a Quadratic Boost Converter (QBC), utilizing the Integral of Time-weighted Absolute Error (ITAE) as the objective function to to attain better voltage control and dynamic performance. The study rigorously evaluated the controller's robustness under multiple operational scenarios, including varying reference voltage (180V, 220V, and 240V) and load resistances (50Ω, 100Ω, and 200Ω).

The PSO algorithm effectively optimized the PI controller gains, ensuring minimal steady-state error, negligible overshoot (< 2%), and rapid transient response across all test conditions. The converter demonstrated exceptional reference tracking accuracy, maintaining the desired output voltage even under sudden load changes, which emphasize the controller's adaptive capability and disturbance rejection properties. Additionally, the ITAE-based optimization helped achieve the best possible balance between damping and response speed, which produced a critically damped-like behavior devoid of noticeable oscillations.

Key performance metrics, including rise time (T_r), settling time (T_{ss}), and percentage overshoot (%M_{pp}), were consistently within acceptable limits, confirming the system's stability and efficiency under dynamic operating conditions. The results also highlighted the scalability of the proposed control strategy, as it performed reliably across a wide range of voltage levels and load variations.

The findings of this research contribute to the advancement of intelligent control strategies for high-gain DC-DC converters, offering a reliable, optimized solution for applications requiring precise voltage regulation, such as electric vehicles, microgrids, and renewable energy systems.

Conflict of interest

There is no conflict to disclose.

ACKNOWLEDGEMENT

I would like to express my deepest gratitude to my research advisor, Prof.Dr. Iwan Setiawan, ST., MT. and Dr. Susatyo Handoko, ST., MT. for their invaluable guidance, insightful feedback, and unwavering support throughout this study. Their expertise and encouragement were instrumental in shaping this work.

Additionally, I extend my appreciation to the authors and researchers whose pioneering work in PSO algorithm and DC-DC converters laid the foundation for this study. Their contributions were crucial in shaping the direction of this research.

REFERENCES

[1]. *2016 IEEE International Conference on Renewable Energy Research and Applications (ICRERA)*. (2016). IEEE.

[2]. Abdolrasol, M. G. M., Hannan, M. A., Hussain, S. M. S., & Ustun, T. S. (2022). Optimal PI controller based PSO optimization for PV inverter using SPWM techniques. *Energy Reports*, *8*, 1003–1011. https://doi.org/10.1016/j.egyr.2021.11.180

[3]. Ahmed, G., Eltayeb, A., Alyazidi, N. M., Imran, I. H., Sheltami, T., & El-Ferik, S. (2024a). Improved particle swarm optimization for fractional order PID control design in robotic manipulator system: A performance analysis. *Results in Engineering*, *24*. https://doi.org/10.1016/j.rineng.2024.103089

[4]. Ahmed, G., Eltayeb, A., Alyazidi, N. M., Imran, I. H., Sheltami, T., & El-Ferik, S. (2024b). Improved particle swarm optimization for fractional order PID control design in robotic manipulator system: A performance analysis. *Results in Engineering*, *24*. https://doi.org/10.1016/j.rineng.2024.103089

[5]. Barrios Aguilar, M. E., Coury, D. V., Reginatto, R., & Monaro, R. M. (2020). Multi-objective PSO applied to PI control of DFIG wind turbine under electrical fault conditions. *Electric Power Systems Research*, *180*(August 2019). https://doi.org/10.1016/j.epsr.2019.106081

[6]. Borin, L. C., Mattos, E., Osorio, C. R. D., Koch, G. G., & Montagner, V. F. (2019). Robust PID Controllers Optimized by PSO Algorithm for Power Converters. *2019 IEEE 15th Brazilian Power Electronics Conference and 5th IEEE Southern Power Electronics Conference, COBEP/SPEC 2019*. https://doi.org/10.1109/COBEP/SPEC44138.2019.9065642

[7]. Das, R., Rashid, H., & Ahmed, I. U. (2018). A comparative analysis of PI and PID controlled bidirectional DC-DC converter with conventional bidirectional DC-DC converter. *3rd International Conference on Electrical Information and Communication Technology, EICT 2017*, *2018-Janua*(December), 1–6. https://doi.org/10.1109/EICT.2017.8275149

[8]. Essaaidi, Mohamed., & El Hani, Soumia. (2015). *Proceedings of 2015 International Conference on Electrical and Information Technologies : (ICEIT 2015)*. IEEE.

[9]. Guangul, F. M., & Chala, G. T. (2019). Solar Energy as Renewable Energy Source: SWOT Analysis. *2019 4th MEC International Conference on Big Data and Smart City (ICBDSC)*, 1–5. https://doi.org/10.1109/ICBDSC.2019.8645580

[10]. Hsieh, Y. P., Chen, J. F., Liang, T. J., & Yang, L. S. (2012). Novel high step-up DC-DC converter with coupled-inductor and switched-capacitor techniques. *IEEE Transactions on Industrial Electronics*, *59*(2), 998–1007. https://doi.org/10.1109/TIE.2011.2151828

[11]. Hsieh, Y. P., Chen, J. F., Yang, L. S., Wu, C. Y., & Liu, W. S. (2014). High-conversion-ratio bidirectional DC-DC converter with coupled inductor. *IEEE Transactions on Industrial Electronics*, *61*(1), 210–222. https://doi.org/10.1109/TIE.2013.2244541

[12]. Hu, X., & Gong, C. (2014). A High Voltage Gain DC–DC Converter Integrating Coupled-Inductor and Diode–Capacitor Techniques. *IEEE Transactions on Power Electronics*, *29*(2), 789–800. https://doi.org/10.1109/TPEL.2013.2257870

[13]. Kirubakaran, A., Jain, S., & Nema, R. K. (2009). A review on fuel cell technologies and power electronic interface. In *Renewable and Sustainable Energy Reviews* (Vol. 13, Issue 9, pp. 2430–2440). https://doi.org/10.1016/j.rser.2009.04.004

[14]. Liaquat, S., Bhatti, O. S., & Janjua, K. A. (2019). Accelerated PSO-Scaled PI Controller for DC-DC Boost Converter in Photovoltaic Systems. *2019 3rd International Conference on Energy Conservation and Efficiency, ICECE 2019 - Proceedings*. https://doi.org/10.1109/ECE.2019.8920851

[15]. Lofthouse, J. (2015). *Reliability of renewable energy: Solar*.

[16]. López-Santos, O., Martínez-Salamero, L., García, G., Valderrama-Blavi, H., & Mercuri, D. O. (2013). Efficiency analysis of a sliding-mode controlled quadratic boost converter. *IET Power Electronics*, *6*(2), 364–377. https://doi.org/10.1049/iet-pel.2012.0417

[17]. Malarvili, S. M., Mageshwari, S. M., & Vinothkumar. (2021). Artificial Intelligent Parameter based PSO for Maximum Power Point Tracking of PV Systems under PSC. *Proceeding - 2021 IEEE 17th International Colloquium on Signal Processing and Its Applications, CSPA 2021*, 86–91. https://doi.org/10.1109/CSPA52141.2021.9377286

[18]. Niknam, T., Kavousifard, A., Tabatabaei, S., & Aghaei, J. (2011). Optimal operation management of fuel cell/wind/photovoltaic power sources connected to distribution networks. *Journal of Power Sources*, *196*(20), 8881–8896. https://doi.org/10.1016/j.jpowsour.2011.05.081

[19]. Nouri, T., Babaei, E., & Hosseini, S. H. (2013). A generalized ultra step-up DC–DC converter for high voltage application with design considerations. *Electric Power Systems Research*, *105*, 71–84. https://doi.org/10.1016/J.EPSR.2013.07.012

[20]. *Optimization of Electrical and Electronic Equipment (OPTIM), 2014 International Conference on*. (2014).

[21]. Qian, W., Cao, D., Cintron-Rivera, J. G., Gebben, M., Wey, D., & Peng, F. Z. (2012). A Switched-Capacitor DC–DC Converter With High Voltage Gain and Reduced Component Rating and Count. *IEEE Transactions on Industry Applications*, *48*(4), 1397–1406. https://doi.org/10.1109/TIA.2012.2199731

[22]. Sahin, E., Ayas, M. S., & Altas, I. H. (2014). A PSO optimized fractional-order PID controller for a PV system with DC-DC boost converter. *16th International Power Electronics and Motion Control Conference and Exposition, PEMC 2014*, 477–481. https://doi.org/10.1109/EPEPEMC.2014.6980539

[23]. Sinha, D., Mahapatra, M. Das, Pal, S., Majumder, S., Bhattacharya, S., & Bandyopadhyay, C. (2025). Adaptation of fractional-order PI controller for a variable input interleaved DC–DC boost converter using particle swarm optimization with parametric variation. *IFAC Journal of Systems and Control*, *32*. https://doi.org/10.1016/j.ifacsc.2025.100301

[24]. Trujillo, C. L., Santamaría, F., & Gaona, E. E. (2016). Modeling and testing of two-stage grid-connected photovoltaic micro-inverters. *Renewable Energy*, *99*, 533–542. https://doi.org/10.1016/j.renene.2016.07.011